Desalination and Water Treatment
www.deswater.com
doi: 10.1080/19443994.2015.1084593

57 (2016) 17283–17290
August

Taylor & Francis
Taylor & Francis Group

Membrane fouling control in the integrated process of magnetic anion exchange and ultrafiltration

Zhaohui Zhang[a,b,*], Qianqian Chen[a], Liang Wang[a,b], Hongwei Zhang[a], Bin Zhao[a,b], Cong Ma[a,b]

[a]*School of Environmental and Chemical Engineering, Tianjin Polytechnic University, Tianjin 300387, P.R. China, Tel./Fax: +86 22 83955163; emails: zzh7448@126.com (Z. Zhang), 1135045569@qq.com (Q. Chen), mashi7822@163.com (L. Wang), hwzhang@tju.edu.cn (H. Zhang), zhao.bin.j@gmail.com (B. Zhao), hit.macong@gmail.com (C. Ma)*
[b]*State Key Laboratory of Separation Membranes and Membrane Processes, Tianjin Polytechnic University, Tianjin 300387, P.R. China*

Received 24 October 2014; Accepted 13 August 2015

ABSTRACT

Magnetic anion exchange (MIEX) has been increasingly concerned owing to its excellent performance for the removal of dissolved organic carbon in the treatment of drinking water. In this study, the ability of ultrafiltration (UF) membrane fouling control was analyzed by different combination processes of MIEX-UF. A single cycle and multi-cycle operations were conducted, and the separated and integrated processes of MIEX-UF were compared. Membrane filtration resistance, removal of organics, and morphologies of the membrane surface were analyzed. The results of the short-term operation did not show any obvious improvement in the membrane fouling control in the separated process (compared to UF alone); however, a marked improvement was obtained in the integrated process. The membrane filtration resistance analysis showed that the cake resistance (R_c) and pore blocking resistance (R_p) in the integrated process were only 52 and 24% of the values in the separated process. The multi-cycle operation demonstrated that the cumulative rate of hydraulically irreversible fouling was 0.0021 in the integrated process and was much lower than that in the separated process (0.0182). The mechanistic analysis shows that in the integrated process, a dynamic layer was formed on the membrane surface by the deposited MIEX beads, which markedly decreased the accumulation of the membrane foulants on the membrane surface and in the membrane pores.

Keywords: Membrane fouling; Magnetic anion exchange; Ultrafiltration membrane; Integrated process

1. Introduction

Ultrafiltration (UF) is a promising process to produce qualified drinking water. The application of ultrafiltration for drinking water production has undergone accelerated development during the past decade. Nevertheless, membrane fouling is one important issue that is a major impediment to the progress of this technology. In particular, irreversible membrane fouling reduces the permeate flux, shortens the membrane life, increases the maintenance cost, and eventually adds additional capital cost for membrane replacement [1].

*Corresponding author.

Pretreatment of the feed water to lower natural organic matter (NOM) has been a useful approach to prevent membrane fouling. Pretreatments such as coagulation, adsorption, and ozonation before membrane filtration have been used to ameliorate membrane fouling and improve effluent water quality. Among these pretreatment processes, coagulation is the most widely used and researched owing to its cost effectiveness and easy operation procedure [2]. Applying coagulation process before UF was found to be very effective in decreasing fouling as well as increasing critical flux, because coagulation can effectively remove membrane foulants such as colloid and hydrophobic organics, change the size, and decrease the impurities level to be rejected by the following membrane [3,4]. Powdered activated carbon (PAC) addition has an excellent removal performance in terms of NOM and turbidity; however, whether or not the process is able to alleviate the membrane fouling in a PAC-UF hybrid process is still a matter of debate [5,6]. Some researchers have reported that PAC addition could effectively mitigate the irreversible membrane fouling and results in significantly higher membrane specific flux by water backwashing [7,8]. Alternatively, some researchers have found that PAC addition was ineffective at decreasing membrane fouling despite enhanced removal of micro-molecular NOM [9,10].

Magnetic ion exchange resin (MIEX) developed by Orica Watercare and the South Australian Water Corporation was specifically designed to remove dissolved organic carbon (DOC). Compared to the traditional anion exchange resin, MIEX has higher settlement rate in water, smaller particle size, and excellent removal ability for NOM. A review of the literature pertaining to the treatment with MIEX reveals its potential to remove a greater amount of DOC and ultraviolet (UV)-absorbing substances than the coagulation and PAC, which removes diverse molecular weight and organic acid fractions of DOC than the coagulation and PAC processes and is also capable of removing bromide [11,12]. The use of MIEX pretreatment to decrease low-pressure membrane (LPM) fouling was also reported in several studies [13,14]. The results obtained in these studies indicated that MIEX pretreatment has a slight effect on decreasing short-term fouling of LPM, but has a positive impact on decreasing the hydraulically irreversible fouling in long-term operation. This may be beneficial to the long-term operation of full-scale LPM systems. Notably, in all these studies, the MIEX adsorption and membrane filtration were performed in two separate reactors, called a separated process of MIEX-UF. However, only a few studies about the integrated process of MIEX-UF are reported, in which the MIEX adsorption and membrane filtration were finished in one reactor. Compared to the separated process, the number of reactors required in the integrated process decreased significantly, leading to smaller occupation area, less investment, and lower operating cost.

The objective of this study was to analyze the difference in the membrane fouling control between the integrated and separated processes. Single cycle and multi-cycle operations were performed for both the processes. Based on the results obtained from the pollutant removal efficiency, membrane resistance analysis, and SEM images, mechanism of the membrane fouling control in the integrated process is proposed.

2. Experimental

2.1. Materials

Raw water was used as the influent of a drinking water treatment plant (Tianjin, China) and immediately transported to the laboratory and stored at 4°C in the dark before use. The characteristics of the raw water are listed in Table 1.

Virgin MIEX was received from Orica Watercare (Denver, CO, Australia) and stored in saturated sodium chloride solution. The resin has a polyacrylic backbone containing magnetic iron oxide (Fe_3O_4) as the magnetic nucleus and is a strong-base anion exchange resin with quaternary amine functional groups. The volumetric anion exchange capacity of MIEX resin is 0.52 milliequivalents (meq) per mL resin. The environmental scanning electron microscopy (E-SEM) images of the hydrated MIEX beads indicate the spherical particles with sizes ranging from ~10 to 200 μm and their rough surfaces having macropores with diameters in the range 1–10 μm (Fig. 1). The resin was rinsed with deionized water before use.

Table 1
Characteristics of raw water

Parameter	Unit	Range
pH	–	7.13–7.62
DOC	mg L^{-1}	3.8–6.6
UV_{254}	cm^{-1}	0.065–0.112
SUVA	L mg^{-1} m^{-1}	9.8–2.9
Turbidity	NTU	2.12–4.03
Conductivity	μs cm^{-1}	502–743
Sulfate	mg L^{-1}	51–134

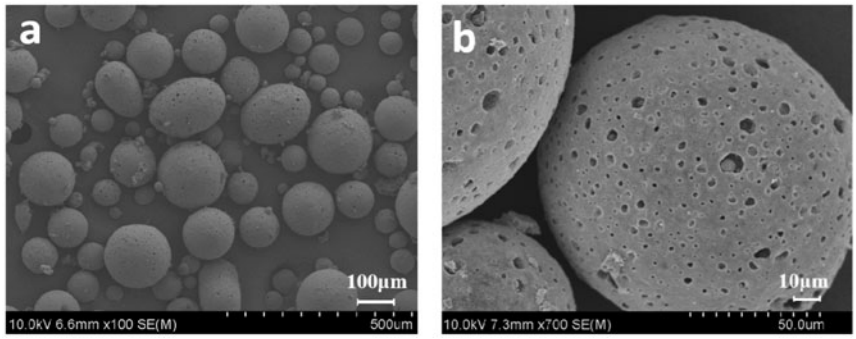

Fig. 1. E-SEM images of virgin MIEX: (a) an overview of MIEX beads (magnification = 100×) and (b) macropores on a resin bead (magnification = 700×).

The UF membrane used in this study was polyvinylidene fluoride (PVDF) hollow fiber membrane, provided by Motimo Membrane Inc. (Tianjin, China). The characteristics of the membrane module used in this study are listed in Table 2.

2.2. Analytical methods

UV_{254} was measured using a spectrophotometer (UV 2550, Shimadzu). DOC concentration in the water was measured with a total organic carbon analyzer (TOC-V_{CPH}, Shimadzu). All the DOC and UV_{254} samples were filtrated through a 0.45-μm microfilter before analysis. Water turbidity was measured using a turbidimeter (2100AN, Hach). Permanganate index (COD_{Mn}) was determined using the standard titrimetric method. All the samples were measured in duplicate with average values reported.

To determine the apparent molecular weight (AMW) distribution of the dissolved organics in water, the UF fractionation method was used. Millipore YM100, YM30, YM10, and YM3 UF membranes were used, and the AMW exclusion limits specified by the manufacturer for these membranes are 100, 30, 10, and 3 kDa, respectively. Water sample was first filtrated through a 0.45-μm microfilter to remove suspended solids. Then, the produced water was filtrated through Millipore YM100, YM30, YM10, and YM3 UF membranes, respectively, in a stirred UF cell (Amicon 8200, Millipore). All the filtrates were collected at a pressure of 55 psi. The DOC of these filtrates was determined using a total organic carbon analyzer. The molecular weight distribution of the dissolved organics in water was obtained by the subtraction method.

Table 2
Characteristics of the hollow fiber membrane module used in the experiments

Item	Characteristics
Material	PVDF
Molecular weight cut-off (MWCO)	150 kDa
Inner diameter	0.7 mm
Outer diameter	1.2 mm
Number of fiber	20
Module type	U-shape membrane module
Length of module	14 cm
Outer surface area	0.0106 m^2

Environmental scanning electron microscope (E-SEM, ProX, Phenom) was used to observe morphology of MIEX and their distribution on the membrane surface. Field emission scanning electronic microscopy (F-SEM, 4800, Hitachi) was used to examine the morphology of the membrane surface.

Resistance analysis:

$$J = \frac{\Delta P}{\mu R_t} \quad (1)$$

$$R_t = R_m + R_c + R_f \quad (2)$$

where J is the permeation flux, ΔP is the transmembrane pressure (TMP), μ is the viscosity of the permeate, R_t is the total resistance, R_m is the intrinsic membrane resistance, R_c is the cake resistance caused by the cake layer on the membrane surface, and R_p is the pore blocking resistance caused by solute adsorption into the membrane pores. Each resistance value can be obtained based on the methods described by Ying et al. and Chang et al. [15,16].

2.3. Experimental systems

The schematic diagram of the experimental system used in this study is shown in Fig. 2. Raw water was pumped into separated and integrated processes of

MIEX-UF with a double-channel peristaltic pump. For the separated process, new MIEX with a dosage of 5 mL/L was continuously fed into the MIEX adsorption tank, where the stirring speed was set at 100 r min^{-1}. DOC in the raw water was adsorbed by MIEX resin. Then, the mixture of water and MIEX was flown into the sedimentation tank, where the MIEX particles settled down quickly and were discharged for regeneration. The supernatant from the sedimentation tank was pumped into the followed membrane filtration tank. In contrast, the MIEX adsorption and membrane filtration are completed in one tank for the integrated process at a stirring speed of 100 r min^{-1} to suspend the MIEX particles. As with the separated process, 5 mL/L new MIEX was continuously added to the tank. Meanwhile, the stirring and filtration were stopped for 5 min every 2 h to settle down and discharge the MIEX particles. The hydraulic retention time for both the MIEX adsorption tank of the separated process and the contact tank of the integrated process was 2 h. The membrane flux was fixed at 50 L m^{-2} h^{-1}, and the vacuum manometer at the produced water side was used to measure the TMP. The membrane model would be backwashed with the effluent water as the TMP increased to 35 kPa.

3. Results and discussion

Fig. 3 shows the TMP profiles of both the processes during one single backwashing cycle and the UF process alone (UF membrane filtration alone without MIEX pretreatment) acting as the control group. The result shows that the pretreatment of MIEX in the separated process has no obvious improvement in the membrane fouling control of UF. The filtration time did not significantly prolong than that of the UF alone. The result was in good agreement with the study by Fabris et al. [17]. However, a marked decrease in the membrane fouling was observed in the integrated process. TMP increased very slowly, and the filtration time lasted for 300 min as the TMP increased to 35 kPa, which was 5 and 3.8 times longer than those of the sole UF and the separated processes, respectively. These results indicate that the membrane

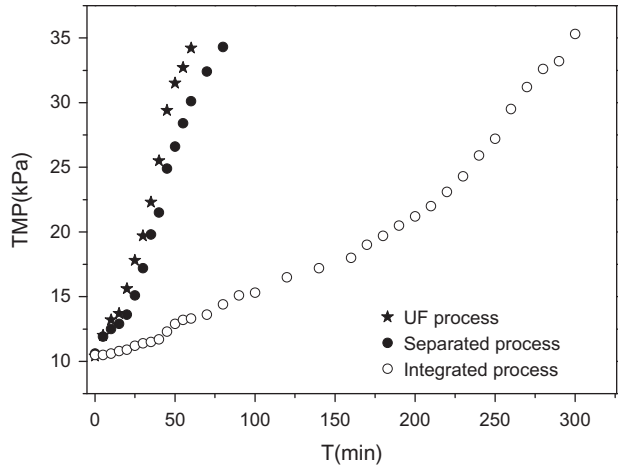

Fig. 3. TMP profiles of MIEX-UF processes in a single backwashing cycle.

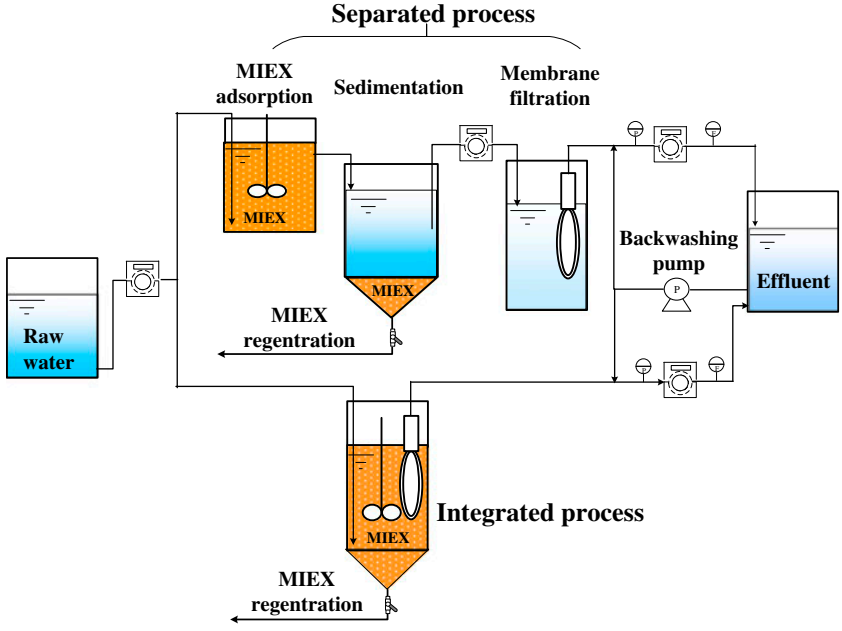

Fig. 2. Schematic diagram of the bench-scale experimental apparatus.

fouling can be effectively controlled in the integrated process instead of the separated process.

To further compare the difference of membrane fouling between the integrated and separated processes, the above experiment was repeated again, and the resistance composition analysis based on the resistance-in-series model was conducted as the filtration has run for 50 min. The corresponding resistances composition and the ratio of resistances were analyzed and calculated as shown in Fig. 4. Obviously, the total resistance (R_t) of the integrated process was much lower than that of the separated process. Moreover, both the cake resistance (R_c) and pore blocking resistance (R_p) in the integrated process were significantly less than those in the separated process. The R_c and R_p in the integrated process were 7.1×10^{11} m^{-1} and 0.58×10^{11} m^{-1}, respectively, which were only 52 and 24% of the values in the separated process. The results, especially a significant decrease in the R_p value for the integrated process, further suggest that the integrated process has more excellent performance than the separated process in hydraulically irreversible fouling control as well as hydraulically reversible fouling control.

Compared to the hydraulically reversible membrane fouling, hydraulically irreversible fouling remains a more serious issue, because it increases chemical cleaning frequency and operational costs, while decreasing the membrane life time [18]. Fig. 5 shows the TMP curves of multi-cycle operation for the integrated process and separated process. The multi-cycle operation lasted for 800 min. During that period, the membranes in the separated and integrated processes were backwashed for 19 and only 3 times, respectively. All the initial TMP data after backwashing were linear fitted for both the processes, respectively. The slope of the linear fitting illustrates the cumulative rate of hydraulically irreversible membrane fouling in the corresponding process [2,19]. Fig. 5 shows that the slope of the linear fitting for the integrated and separated processes was 0.0021 and 0.0182, respectively. The results indicate that the cumulative rate of irreversible membrane fouling in the integrated process was 8.7 times lower than that in the separated process, confirming that integrated process for hydraulically irreversible membrane fouling control was markedly superior to that of the separated process.

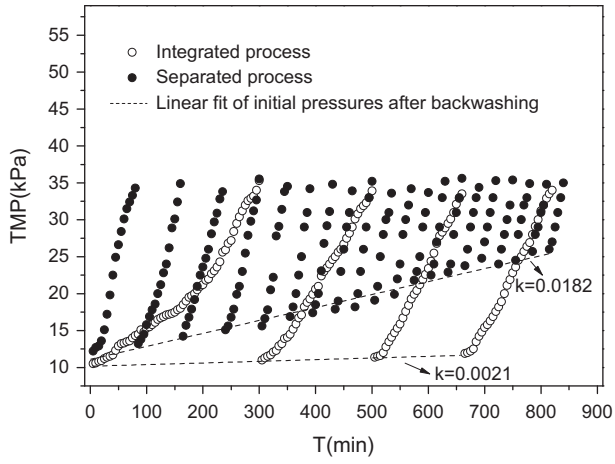

Fig. 5. Irreversible membrane fouling control by MIEX-UF processes.

Based on the membrane resistance analysis, mechanism of the membrane fouling control in the integrated process was further investigated. First, NOM

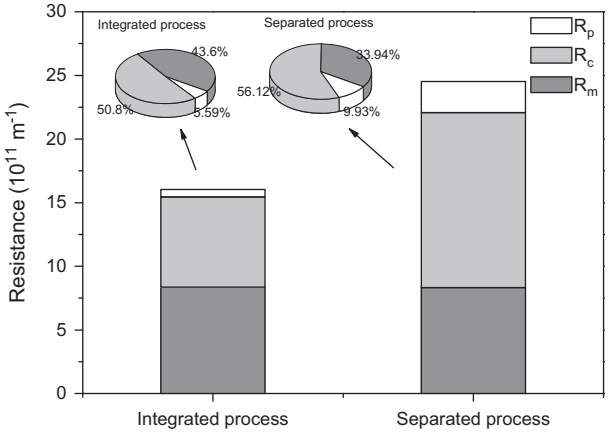

Fig. 4. Membrane filtration resistance analysis of MIEX-UF processes.

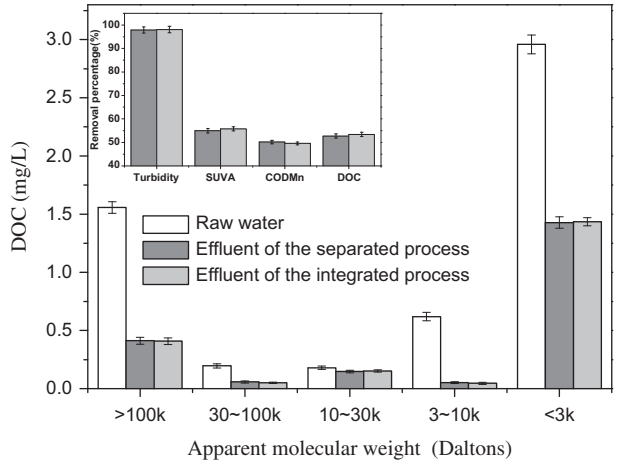

Fig. 6. Water purification performance of the MIEX-UF processes.

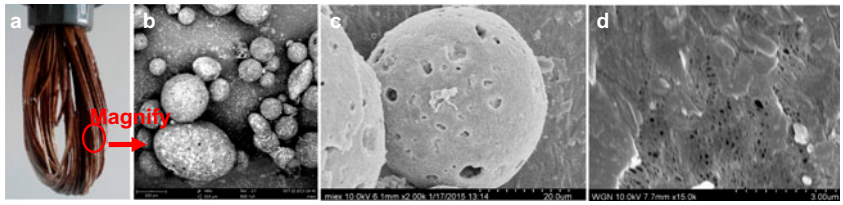

Fig. 7. The MIEX distribution on the membrane surface in the integrated process (a) the membrane module after operated for 800 min, (b) E-SEM images of MIEX beads distribution on the membrane surface (magnification = 440×), (c) the deposited MIEX beads covered by lots of pollutants (magnification = 2000×), and (d) the membrane surface where the MIEX bead was stripped off (magnification = 15,000×).

was identified as dominant membrane foulant in the literature, and the removal of organic pollutants by MIEX in the liquid phase of the integrated reactor probably was the main reason for the membrane fouling control. However, the results in Fig. 6 show that the speculation was untenable, because in each molecular weight range, almost equal amount of organic matter was removed by both the processes. In addition, no obvious difference was observed in the removal of total organic pollutants, suspended solids, and aromatic compounds for both the processes. Therefore, the high efficiency of membrane fouling control for the integrated process should be closely associated with the behavior of the MIEX particles on the membrane surface instead of the removal of organic matter by MIEX in the liquid phase.

Fig. 7(a) shows the image of the membrane module after operated for 800 min in the integrated process. The outer surface of the membrane fibers was coated with the MIEX beads after long-time operation. The layer of MIEX beads played a role of dynamic layer on the membrane surface. When the membrane module was backwashed, the layer of MIEX beads was flushed away from the membrane surface. However, it reformed again soon on the membrane surface as the filtration resumed. Fig. 7(b) shows the MIEX beads distribution on the membrane surface. A competitive adsorption for organic matters between the deposited MIEX and the membrane surface occurred as these organic matters pass through the UF membrane. The deposited MIEX beads have a stronger affinity for NOM than the UF membrane, because they can adsorb these organic matters by ion exchange. As a result, more organic pollutants were intercepted by the deposited MIEX beads instead of the UF membrane surface or pores. Fig. 7(c) shows that the surface of the deposited MIEX bead was covered by lots of pollutants. Fig. 7(d) shows that the membrane pores covered by the deposited MIEX beads were clearly visible as these MIEX beads were stripped off with a needle, indicating that these membrane pores would recover their filtering performance as the membrane was backwashed.

In contrast, in the integrated process, the cake layer formed on the membrane surface consists of the deposited MIEX beads and intercepted pollutants, which probably lead to a looser cake layer than that of the separated process. A marked decrease in the R_c value for the integrated process confirmed the speculation, because the looser cake layer would result in lower cake resistance. Moreover, during hydraulic backwashing, the deposited MIEX beads would be flushed off from the membrane surface and can produce a carrying effect for the whole cake layer. As a result, the cake layer was easier to be removed by backwashing in the integrated process than that in the separated process.

Fig. 8 shows the F-SEM images of the membrane surface before and after backwashing at the end of the operation. It should be mentioned that for the membrane of the integrated process, the deposited MIEX beads on the membrane surface were stripped off using a needle to observe the membrane pores before backwashing. As shown in Fig. 8, for the membrane of the separated process, significant amounts of intercept pollutants accumulated on the membrane surface and membrane pores were invisible before backwashing. In contrast, some membrane pores were still observed clearly for the membrane surface in the integrated process. After backwashing, some pollutants still remained on the membrane surface in the separated process, but almost no remnants were observed on the membrane surface in the integrated process. These F-SEM images further demonstrate that the accumulation of hydraulically irreversible membrane foulants on the membrane surface can be effectively decreased by the integrated process.

Based on the above study, it can be concluded that in the integrated process, the dynamic layer formed by the deposited MIEX beads on the membrane surface plays a critical role in alleviating membrane fouling; however, further discussion about the mechanism will be conducted in the near future.

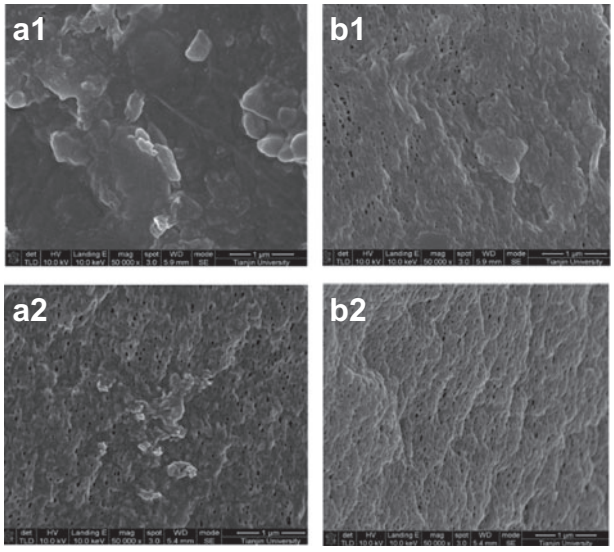

Fig. 8. F-SEM images of membrane surface before and after backwashing (magnification = 50,000×): (a) the membrane surface in the separated process and (b) the membrane surface in the integrated process; (1) before backwashing; (2) after backwashing.

4. Conclusions

UF membrane fouling control in the separated and integrated processes of MIEX-UF was investigated in this study. Compared to the UF alone, poor efficiency was observed for membrane fouling control in the separated process, but excellent performance was obtained in the integrated process. The membrane resistance analysis and multi-cycle operation suggest that hydraulically reversible membrane fouling, especially hydraulically irreversible membrane fouling, can be effectively decreased in the integrated process. The mechanistic analysis indicates that the membrane fouling control in the integrated process should be closely related to the dynamic layer formed by the deposited MIEX beads on the membrane surface, but was not associated with the removal of organics by MIEX in the liquid phase of the reactor.

Supplementary material

The supplementary material for this paper is available online at http://dx.doi.10.1080/19443994.2015.1084593.

Acknowledgements

This study was financially supported by the National Natural Science Foundation of China (51308391, 21206125, 51478314, 51138008, and 51308390), Tianjin Science and Technology Program (14ZCDGSF00128) and Tianjin Natural Science Fund (14JCQNJC0900).

References

[1] H. Yamamura, S. Chae, K. Kimura, Y. Watanabe, Transition in fouling mechanism in microfiltration of a surface water, Water Res. 41 (2007) 3812–3822.
[2] K. Kimura, T. Maeda, H. Yamamura, Y. Watanabe, Irreversible membrane fouling in microfiltration membranes filtering coagulated surface water, J. Membr. Sci. 320 (2008) 356–362.
[3] C.W. Jung, H.J. Son, L.S. Kang, Effects of membrane material and pretreatment coagulation on membrane fouling: fouling mechanism and NOM removal, Desalination 197 (2006) 154–164.
[4] W. Gao, H. Liang, J. Ma, M. Han, Z.L. Chen, Z.S. Han, G.B. Li, Membrane fouling control in ultrafiltration technology for drinking water production: A review, Desalination 272 (2011) 1–8.
[5] Y.H. Li, X.J. Zhang, W. Zhang, J. Wang, C. Chen, Effect of powdered activated carbon on immersed hollow fiber ultrafiltration membrane fouling caused by particles and natural organic matter, Desalination 278 (2011) 443–446.
[6] Y. Matsui, H. Hasegawa, K. Ohno, T. Matsushita, S. Mima, Y. Kawase, T. Aizawa, Effects of superpowdered activated carbon pretreatment on coagulation and trans-membrane pressure buildup during microfiltration, Water Res. 43 (2009) 5160–5170.
[7] K. Li, F.S. Qu, H. Liang, S.L. Shao, Z.S. Han, H.Q. Chang, X. Du, G.B. Li, Performance of mesoporous adsorbent resin and powdered activated carbon in mitigating ultrafiltration membrane fouling caused by algal extracellular organic matter, Desalination 336 (2014) 129–137.
[8] M.M.T. Taimur Khan, S. Takizawa, Z. Lewandowski, M.H. Habibur Rahman, K. Komatsu, S.E. Nelson, F. Kurisu, A.K. Camper, H. Katayama, S. Ohgaki, Combined effects of EPS and HRT enhanced biofouling on a submerged and hybrid PAC-MF membrane bioreactor, Water Res. 47 (2013) 747–757.
[9] M.B. Dixon, Y. Richard, L. Ho, C.W.K. Chow, B.K. O'Neill, G. Newcombe, A coagulation-powdered activated carbon-ultrafiltration-multiple barrier approach for removing toxins from two Australian cyanobacterial blooms, J. Hazard. Mater. 186 (2011) 1553–1559.
[10] J. Lohwacharin, K. Oguma, S. Takizawa, Use of carbon black nanoparticles to mitigate membrane fouling in ultrafiltration of river water, Sep. Purif. Technol. 72 (2010) 61–69.
[11] H. Humbert, H. Gallard, H. Suty, J.P. Croué, Natural organic matter (NOM) and pesticides removal using a combination of ion exchange resin and powdered activated carbon (PAC), Water Res. 42 (2008) 1635–1643.
[12] T.H. Boyer, P.C. Singer, A pilot-scale evaluation of magnetic ion exchange treatment for removal of natural organic material and inorganic anions, Water Res. 40 (2006) 2865–2876.
[13] R. Zhang, S. Vigneswaran, H. Ngo, H. Nguyen, A submerged membrane hybrid system coupled with magnetic ion exchange (MIEX®) and flocculation in wastewater treatment, Desalination 216 (2007) 325–333.

[14] H.O. Huang, H.H. Cho, K.J. Schwab, J.G. Jacangelo, Effects of magnetic ion exchange pretreatment on low pressure membrane filtration of natural surface water, Water Res. 46 (2012) 5483–5490.
[15] Z. Ying, G. Ping, Effect of powdered activated carbon dosage on retarding membrane fouling in MBR, Sep. Purif. Technol. 52 (2006) 154–160.
[16] I.S. Chang, C.H. Lee, Membrane filtration characteristics in membrane-coupled activated sludge system-the effect of physiological states of activated sludge on membrane fouling, Desalination 120 (1998) 221–233.
[17] R. Fabris, E.K. Lee, C.W.K. Chow, V. Chen, M. Drikas, Pre-treatments to reduce fouling of low pressure micro-filtration (MF) membranes, J. Membr. Sci. 289 (2007) 231–240.
[18] S. Peldszus, C. Hallé, R.H. Peiris, M. Hamouda, X.H. Jin, R.L. Legge, H. Budman, C. Moresoli, P.M. Huck, Reversible and irreversible low-pressure membrane foulants in drinking water treatment: Identification by principal component analysis of fluorescence EEM and mitigation by biofiltration pretreatment, Water Res. 45 (2011) 5161–5170.
[19] K. Kimura, H. Yamamura, Y. Watanabe, Irreversible fouling in MF/UF membranes caused by natural organic matters (NOMs) isolated from different origins, Sep. Sci. Technol. 41 (2006) 1331–1344.